On the relevance of the coupling model to experiments

2007 J. Phys.: Condens. Matter 19 205114

(http://iopscience.iop.org/0953-8984/19/20/205114)

IOP PUBLISHING JOURNAL OF PHYSICS: CONDENSED MATTER

J. Phys.: Condens. Matter **19** (2007) 205114 (25pp) doi:10.1088/0953-8984/19/20/205114

On the relevance of the coupling model to experiments

K L Ngai[1] **and S Capaccioli**[2,3]

[1] Naval Research Laboratory, Washington, DC 20375-5320, USA
[2] Dipartimento di Fisica, Università di Pisa, Largo B Pontecorvo 3, I-56127, Pisa, Italy
[3] CNR-INFM, CRS SOFT, Piazzale Aldo Moro 2, 00185, Roma, Italy

Received 9 October 2006
Published 25 April 2007
Online at stacks.iop.org/JPhysCM/19/205114

Abstract

The research field of the glass transition is experimentally driven. There is an abundance of experimental data and facts accumulated in the past as well as the emergence of important new results every now and then. Therefore, when judging theories and models of the glass transition, it is fair to ask the question of their relevance to experiments. This question was one of the themes of a round-table discussion session entitled *An assessment of current theories: interconnections and relevance to experiments*, organized at the 4th Workshop on Non-equilibrium Phenomena in Supercooled Fluids, Glasses and Amorphous Materials (4th WNEP). The coupling model has a history of making connections of its theoretical results with many experimental facts on dynamics of glass-forming substances. This characteristic of the coupling model is demonstrated herein by using it to explain or rationalize some of the new experimental data reported at the 4th WNEP and published in this volume and elsewhere.

(Some figures in this article are in colour only in the electronic version)

1. Introduction

At the 4th Workshop on Non-equilibrium Phenomena in Supercooled Fluids, Glasses and Amorphous Materials (4th WNEP), the papers presented were very stimulating. Two round-table discussion sessions were organized to discuss issues that impact on our current understanding or lack of understanding of the dynamics of the glass transition. Round Table 2 was organized by P G Debenedetti and H Z Cummins. It was entitled *An assessment of current theories: interconnections and relevance to experiments*. As one of the discussion leaders, one of us (KLN) spoke on the coupling model (CM) [1–8]. Since the emphasis of the discussion was on relevance of theory to experiments, some examples of many previously published applications of the CM to explain experimental data were given. Indeed, relevance to experiments is the strength of the CM, as demonstrated by its ability to rationalize, explain, and sometimes predict dynamics properties before verifications by experiments. A number of papers presented at the 4th WNEP provide new experimental and simulation data that challenge any theory to explain. In this paper, we demonstrate once more the relevance of the CM to experiments by explaining some of these fresh experimental and simulation data, some of which

had not yet been published when reported at the 4th WNEP but will appear as published papers in this volume and elsewhere.

2. Invariance of the ratio τ_{JG}/τ_α for different T and P when τ_α is kept constant

Recent advances in experimental techniques including broadband dielectric relaxation and light scattering have made possible measurements of structural relaxation (local segmental relaxation in the case of polymers) in glass-forming substances under applied pressure typically up to a few GPa. The dielectric relaxation and photon correlation spectroscopy data for more than 30 polymeric and small molecular glass-formers (excluding those with hydrogen bonds) show that the time/frequency dispersion of the structural α-relaxation is invariant for various combinations of pressure P and temperature T when its most probable structural relaxation time τ_α or frequency ν_α is constant [9, 10]. The α-dispersions are uniquely and well described in the time domain by the Kohlrausch functions,

$$\phi(t) = \exp[-(t/\tau_\alpha)^{1-n}], \tag{1}$$

with the following caveat. When fitting the frequency dependence of the α-loss peaks obtained by dielectric relaxation by the one-sided Fourier transform of the Kohlrausch function, emphasis of good agreement with the loss data is on the main peak, especially the low-frequency side, if no significant conductivity contribution is present there, or has been removed if present. This fit has taken into account nearly all the dielectric or mechanical strength of the α-relaxation and the viscosity if the glass-former is not polymeric. Deviations of the Kohlrausch fit to the data invariably occur at frequencies sufficiently high above the loss maximum. The deviations are considered natural in the coupling model (CM) interpretation of the evolution of dynamics with time [6–8]. They come from processes of smaller length-scales that transpire at shorter times before the dynamics evolve to the one with maximum length-scale and correlation function given by the Kohlrausch function. Thus, the experimental fact of constant dispersion at constant τ_α for different T and P can be restated as the invariance of the fractional exponent n (or the Kohlrausch exponent, $\beta_{KWW} \equiv 1 - n$), which determines the breadth of the dispersion. In other words, τ_α and n (or β_{KWW}) are co-invariants of changing thermodynamic conditions (T and P). This remarkable finding has an immense impact on the glass transition. This is because theories or models of the glass transition, in which the dispersion of the structural relaxation is not one of the determining factors of the structural relaxation time, are unlikely to be consistent with this property by coincidence. An exception is the coupling model (CM) [1–8], whose defining equation,

$$\tau_\alpha = [t_c^{-n}\tau_0]^{1/(1-n)}, \tag{2}$$

links together τ_α and the dispersion parameter n; that is, the relationship between the two quantities is fundamental to the CM. The crossover time t_c of the CM is determined by the interaction potential and is independent of T and P. Nevertheless, equation (2) can be fully consistent with the observed co-invariance of τ_α and n only if the primitive relaxation time τ_0 is simultaneously invariant to different T and P. To test this, we make use of the similar nature of the theoretical primitive relaxation and the experimentally observed Johari–Goldstein (JG) secondary relaxation, which leads to the expectation that their relaxation times are approximately equal, i.e., $\tau_0 \approx \tau_{JG}$. This relation has been shown to hold for many glass-formers by data taken at ambient pressure [6–8, 10, 11], whereby τ_0 calculated from the experimental quantities τ_α and n of the α-relaxation by equation (2) is indeed approximately the same as the JG relaxation time τ_{JG}. Thus, a critical test of the CM's explanation of the co-invariance of τ_α and n is the simultaneous invariance of τ_{JG} to different T and P. Glass-formers

having smaller n have smaller separation between $\log \tau_\alpha$ and $\log \tau_0$ (or $\log \tau_{JG}$) according to equation (2). As a result, the JG relaxation is not resolved and it appears as an excess wing on the high-frequency flank of the α-loss peak. Dielectric relaxation experiments carried out at elevated pressures up to 2 GPa and high temperatures to compare with data taken at ambient pressure of 0.1 MPa have shown the shape of the entire dispersion including the α-loss peak, and the excess wing remains unchanged at constant τ_α [9, 10, 12]. Of course, the intensities or strengths of the two processes may have different T- and P-dependences and they are responsible for slight deviation from perfect superposition of the data at high frequencies. These experimental data already provide experimental support of the co-invariance of τ_α, n, and τ_{JG}, or equivalently the co-invariance of τ_α, n, and τ_0 as predicted by the CM. Nevertheless, it would be more complete and convincing if one can observe the co-invariance of τ_α, n, and τ_{JG} in glass-formers that have a resolved JG secondary relaxation. Such new data in which the JG relaxation has been resolved in the liquid state and below T_g were reported at the 4th WNEP by Capaccioli and co-workers [13] in the neat glass-former benzoin-butyl-ether (BIBE) [9, 10] and quinaldine in mixtures with tri-styrene [13], and by Prevosto *et al* [14] in polyphenylglycidylether (PPGE), diglycidyl ether of bisphenol-A (DGEBA), and dipropylene glycol dibenzoate (DPGDB). Co-invariance of τ_α, n, and τ_{JG} for different T and P were found in these neat glass-formers and a component (quinaldine) in binary mixtures. This is a remarkable experimental fact that challenges any theory to explain, but is fully consistent with the CM. In addition, the calculated τ_0 is in agreement with the observed τ_{JG} within experimental uncertainty in all cases. The new results verify the CM explanation (equation (2)) of the invariance of the α-dispersion at constant τ_α for different T and P.

3. The α-dispersion of a component in binary polymer blends is invariant to T and P when τ_α is constant

Roland *et al* [15, 16] reported a dielectric spectroscopic study of the component dynamics in the miscible blend of poly(vinyl methyl ether) (PVME) and poly(2-chlorosytrene) (P2CS). For the PVME component (which has the more intense loss peak due to its higher polarity), the shape of the segmental relaxation loss peak depends only on the relaxation time and is otherwise independent of thermodynamic conditions, i.e., different P and T combinations. The same result was obtained before by Alegria *et al* [17] for the PVME component in the miscible blend of PVME with polystyrene (PS). This property of the component dynamics of miscible polymer blends is in accord with the general behaviour of neat materials discussed in the preceding section. Several models have been proposed to address the component dynamics of polymer blends [18–20]. None of these models except that based on the CM model [21–27] consider the dispersion of the α-relaxation of a component in the blend (or in its neat state), and naturally these models cannot address the observation of the invariance of the dispersion of the segmental relaxation of the component PVME for different T and P at constant relaxation time. On the other hand, the CM for component dynamics of polymer blends is based on considering the dispersion of the segmental relaxation of the component in different environments i due to composition or concentration fluctuations. As discussed in detail in published works [21–26], the segmental relaxation in environment i with relaxation time $\tau_{\alpha i}$ has its own coupling parameter n_i, and the corresponding Kohlrausch function with stretch exponent, $(1 - n_i)$, determines the dispersion. In the same manner as shown for neat glass-formers in the preceding section, the CM ensures co-invariance of $\tau_{\alpha i}$ and n_i (or the shape of the loss peak contributed by i) for different T and P. The observed segmental relaxation of the component is composed of contributions from all i, and hence its shape depends only

on the relaxation time and is otherwise independent of thermodynamic conditions (T and P combinations), as observed for PVME in two different blends.

The property of the dynamics of a component in polymer blends discussed in the paragraph above is also found in mixtures of two small molecular glass-formers as reported by Capaccioli [13]. The systems he studied by dielectric spectroscopy at ambient and elevated pressure are mixtures of 5% and 10% quinaldine with tri-styrene. Since the dipole moment of quinaldine is much larger than that of tri-styrene, the observed spectra are contributed effectively by the motions of quinaldine. In each mixture, the shape of the α-loss peak of quinaldine is invariant to T and P when τ_α is held constant, just like PVME in blends with P2CS and PS. The invariance of the shape was found to hold for more than one constant τ_α value. Moreover, as mentioned in the previous section, $\tau_{\rm JG}$ of the quinaldine component is also invariant to T and P when τ_α is kept constant, and is in agreement with the calculated τ_0.

4. Changing separation of the JG relaxation from the α-relaxation of the faster component with composition of the blends and mixtures

There are examples other than the ones discussed in the previous section that show that the component dynamics of binary polymer blends and binary mixtures of molecular glass-formers are similar. Another one is the increasing separation between the α-relaxation and the JG relaxation of the faster component, measured by $(\log \tau_\alpha - \log \tau_{\rm JG})$ at constant τ_α, with increasing concentration of the slower component in a blend or mixture. For mixtures of small molecular glass-formers, this was seen in picoline mixed with tri-styrene or *ortho*-terphenyl by Blochowicz and Rössler [28] and discussed in [26], as well as in quinaldine when mixed with tri-styrene or low molecular weight polystyrene [13]. This trend is in agreement with the prediction $(\log \tau_\alpha - \log \tau_{\rm JG}) \approx n(\log \tau_\alpha + 11.7)$, which follows from the CM equation (2), and the expected increase of n_i of the faster component with increasing presence of the slower component. Concentration fluctuations are inevitably present in mixtures. They cause additional broadening of the α-relaxation of the faster component and a distribution of n_i, making it impossible to extract even the most probable $\hat{n}$ by fitting the observed α-dispersion of the faster component by the Kohlrausch function, unlike the case of pure glass-formers. Fortunately, at sufficiently low concentration of the faster component, the additional broadening by concentration fluctuations is minimized. The fit gives a good estimate of $\hat{n}$, which can be used to calculate the τ_0 and hence $\tau_{\rm JG}$ from the relation $\tau_0 \approx \tau_{\rm JG}$ of that faster component in the mixture. This procedure was carried out for the mixture of 5% quinaldine with tri-styrene [13], and the calculated τ_0 is in agreement with $\tau_{\rm JG}$ of the observed JG relaxation coming from quinaldine.

For polymer blends, examples include the component PVME blended with PS [29], where the unresolved JG relaxation of neat PVME become resolved on addition of PS (it is worthwhile mentioning that the two resolved secondary relaxations of neat PVME, located below 120 K at 1 Hz, are not the JG relaxation; instead they originate from intramolecular degrees of freedom). The situation is like picoline or quinaldine in tristyrene, where the JG relaxation of picoline and quinaldine are unresolved in the pure state but becomes resolved with addition of tri-styrene [13, 26, 28]. The appearance of the JG relaxation of PVME in the isochronal spectra is particularly clear when more than 50% of PS is present in the blends. For example, see the data for 70% PS in figure 3 of [29a] and the coloured figure 2 of [29b] where both the α- and the JG β-relaxations of PVME are evident in the isochronal loss spectrum at 1 Hz. The authors of [29a] gave in their figure 1(b) the temperature of about 280 K at which the α-relaxation frequency is 1 Hz, while from their figure 7 we can see that the JG β-relaxation frequency is 1 Hz at about 225 K. The α-relaxation time increases much more than the JG

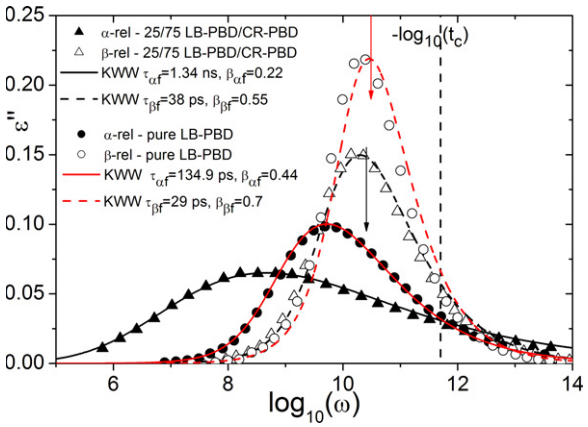

Figure 1. Normalized dielectric loss contributions due to α- and β-relaxation processes of LB-PBD in the pure melt (closed and open circles respectively) and the 25/75 LB-PBD/CR-PBD blend (closed and open triangles respectively) at 198 K obtained by Bedrov and Smith [31b]. The lines are fits by one-sided Fourier transforms of Kohlrausch functions. The vertical arrows indicate the angular frequencies, $\omega_{\beta f} \equiv 1/\tau_{\beta f}$, where $\tau_{\beta f} = \tau_{0f}$ and τ_{0f} are calculated by the appropriate CM equation (see text).

relaxation time of the PVME with increasing PS content. Thus, the separation between the α-relaxation and the JG relaxation of PVME, measured by $(\log \tau_\alpha - \log \tau_{\rm JG})$ at constant τ_α, increases with increasing concentration of PS in the PVME/PS blends. Another example is poly(ethyl methacrylate) (PEMA) blended with poly(4-vinylphenol) [30]. Neat PEMA has a resolved JG relaxation, which continues to be observed in the blend. When PEMA is blended with the slower poly(4-vinylphenol), $(\log \tau_\alpha - \log \tau_{\rm JG})$ of the PEMA component is observed to increase at constant τ_α [30].

Another similar example is given by molecular dynamics simulations of model miscible polymer blends consisting of chemically realistic 1,4-polybutadiene (CR-PBD) as the slow component (higher $T_{\rm g}$) and PBD chains with reduced dihedral barriers as the fast component (LB-PBD) with lower $T_{\rm g}$ by Bedrov and Smith [31]. The simulation was designed to study the influence on the segmental α-relaxation and the JG β-relaxation of the fast component when mixed with the slow component. Before blending, the relaxation times of the α- and JG β-relaxations of the neat fast component are too close together, so the faster but weaker JG β-relaxation cannot be easily resolved (like neat picoline, quinaldine or PVME). However, with addition of the slow component, they found a monotonic increase in the separation between the α- and the JG β-relaxations of the fast component, whereby the latter becomes resolved. The increased separation between the two is due to the strong increase of the α-relaxation time, $\tau_{\alpha f}$, of the fast component (accompanied by an increase of breadth of the α-dispersion or decrease of the stretch exponent, $\beta_\alpha \equiv 1 - n_f$, of the Kohlrausch function used to fit the correlation function; see figure 1) with increasing concentration of the slow component, concomitant with a much smaller change of the relaxation time, $\tau_{\beta f}$, of the β-relaxation of the fast component. These results from simulations by Bedrov and Smith are fully compatible with the experimental data for polymer blends and mixtures mentioned above and the explanation by the CM as shown in a recent comment on Bedrov and Smith by us [32] and figure 1. The decrease of β_α and the concomitant increase of the separation between $\tau_{\alpha f}$ and $\tau_{\beta f}$ with increase in the concentration of the slower CR-PBD are consistent with the prediction of the CM due to increase of the coupling parameters n_{fi}. Bedrov and Smith [31b] tested the CM quantitatively

by using their parameters obtained from their fits of the dipole moment autocorrelation function of the fast LB-PBD component, $\mathrm{DACF}_{(f)}(t) = A_\beta \exp[-(t/\tau_{\beta f})^{\beta_{\beta f}}] + A_\alpha \exp[-(t/\tau_{\alpha f})^{\beta_{\alpha f}}]$. From the relaxation times, $\tau_{\alpha f}$ and $\tau_{\beta f}$, obtained by simulation, they used the CM relations, $\tau_{\alpha f} = [t_c^{-\hat{n}_f}\tau_{0f}]^{1/(1-\hat{n}_f)} \approx [t_c^{-\hat{n}_f}\tau_{\beta f}]^{1/(1-\hat{n}_f)}$, to calculate the most probable $\hat{\beta}_{\alpha f} \equiv 1 - \hat{n}_f$ and compare it with $\beta_{\alpha f}$ from their fit to the DACF. The crossover time t_c of the CM is not available from the simulation, and 2 ps is assumed to be its value as experimentally found for polymers [31b]. The $\hat{\beta}_{\alpha f}$ calculated by Bedrov and Smith are significantly larger than $\beta_{\alpha f}$ for blends with 10, 25, 50, 75 and 100% of the fast component as shown in figure 6 of [31b], which would suggest that the CM prediction is not in quantitative agreement with molecular dynamics simulation. This failure of the CM for simulation data may cast doubt on the quantitative success of the CM in explaining the dynamics of the fast component in dielectric relaxation experiments on real mixtures [13]. However, we point out that there is an important difference between the two cases. In dielectric experiment, τ_{0f} is long compared with $t_c = 2$ ps and in this case the relation, $\tau_{\alpha f} = [t_c^{-\hat{n}_f}\tau_{0f}]^{1/(1-\hat{n}_f)} \approx [t_c^{-\hat{n}_f}\tau_{\beta f}]^{1/(1-\hat{n}_f)}$, obtained by using the continuity of the correlation function across t_c, is applicable. On the other hand, $\tau_{\beta f}$ from simulation (and hence also τ_{0f}) is only a little more than a decade longer than $t_c = 2$ ps, and moreover $\hat{n}_f$ is exceedingly large in blends rich in CR-PBD. In this case, one should use the relation, $\tau_{\alpha f} = [(1-\hat{n}_f)t_c^{-\hat{n}_f}\tau_{0f}]^{1/(1-\hat{n}_f)} \approx [(1-\hat{n}_f)t_c^{-\hat{n}_f}\tau_{\beta f}]^{1/(1-\hat{n}_f)}$, obtained by using the continuity of relaxation rate across, t_c [1], which will be shown elsewhere [31c]. Thus, these equations of the CM should be used to test the simulation data against the CM. In figure 1, we demonstrate such a test for the pure LB-PBD and 25% LB-PBD blend. Normalized dielectric losses from the α- and β-relaxations of the fast LB-PBD in the pure melt and in the 25LB-PBD/75CR-PBD blend from simulation at 198 K are shown (same as figure 8 in [31b]). The one-sided Fourier transform of the Kohlrausch function, $\exp[-(t/\tau_{\alpha f})^{\beta_{\alpha f}}]$, that fits well the frequency dependence of α-relaxation loss peak have parameters $\{\tau_{\alpha f} = 1.34$ ns, $\beta_{\alpha f} = 0.22\}$ for the 25LB-PBD/75CR-PBD blend, and $\{\tau_{\alpha f} = 134.9$ ps, $\beta_{\alpha f} = 0.44\}$ for the pure LB-PBD melt. From these parameters, we calculate $\tau_{\beta f}$ from the appropriate relation, $\tau_{\beta f} = \tau_0 = [(1-\hat{n}_f)^{-1}(t_c)^{\hat{n}_f}(\tau_{\alpha f})^{1-\hat{n}_f}]$, where $t_c = 2$ ps and $(1-\hat{n}_f) = \beta_{\alpha f}$. The last relation is justified by the negligible concentration fluctuation found in these blends [31d]. The reciprocal $\omega_{\beta f} \equiv 1/\tau_{\beta f}$ of the calculated value of $\tau_{\beta f}$, shown in figure 1 by the location of the vertical arrow, is in good agreement with the angular frequency of the LB-PBD β-relaxation loss peak for the 25LB-PBD/75CR-PBD blend as well as for the pure LB-PBD melt. Similar good agreements have been found for the other blend compositions [31c] within the uncertainties or errors involved in deducing the parameter values from the data by Bedrov and Smith with the assumption that the α- and β-relaxations are additive in composing the DACF. Thus, it seems that the CM fares reasonably well in explaining quantitatively the simulation results.

The simulation data also provide information on the slower CR-PBD component in the blend. The α-relaxation time of the slower CR-PBD component becomes shorter, and interestingly its frequency dispersion becomes *narrower* when compared with that of neat CR-PBD. In [32], it is pointed out that this simulation result is also consistent with the prediction of the CM of relaxation on the slower component. At low LB-PBD content in the blend, broadening of the α-relaxation by concentration fluctuations is not that important, and hence the narrowing caused by reduction of the coupling parameter of CR-PBD dominates and it shows up in the simulation data of Bedrov and Smith. In fact, reduction of n of a slower (higher T_g) component when blended with a faster (lower T_g) component had been seen before for sorbitol or xylitol in mixtures with water [25] and sorbitol mixed with glycerol [24] and explained by using the CM.

5. Can anyone reliably predict quantitatively the segmental relaxation time of a component in a polymer blend?

Several papers presented at the 4th WNEP are concerned with the dynamics of a component polymer in binary polymer blends. The current vogue is to compare the segmental relaxation time of a component with the Lodge–McLeish model [20], which stresses the importance of the effect of self-concentration of a polymer in accounting for concentration fluctuations. Composition fluctuations in polymer blends are different from mixtures of small molecular glass-former. In polymer blends, a component has more repeat units of its own kind nearby due to chain connectivity. This is correctly pointed out by Lodge and McLeish (LM). They went on to suggest that the local composition is altered from the average value ϕ to an effective concentration, $\phi_{\rm eff} = \phi_{\rm self} + (1 - \phi_{\rm self})\phi$, where $\phi_{\rm self}$ accounts for the excess of segments due to the chain connectivity. The modified Fox equation, $T_{\rm g}(\phi) = [\phi_{\rm eff}/T_{\rm g1} + (1 - \phi_{\rm eff})/T_{\rm g2}]^{-1}$, is then used to obtain $T_{\rm g}(\phi)$ of the component. The segmental relaxation time in the blend, $\tau_{\rm seg}(\phi)$, is calculated by modifying the Vogel–Fulcher–Tammann–Hesse (VFTH) equation obtained for the component when it is in its neat state, $\tau_{\rm seg} = \tau_\infty \exp[B/(T - T_0)]$, by only replacing T_0 by $T_0(\phi)$. Here $T_0(\phi) = T_0 + [T_{\rm g}(\phi) - T_{\rm g}]$. In other words, the difference between T_0 (ϕ) of component in the blend and T_0 of the neat polymer is exactly the same as the difference between $T_{\rm g}$ (ϕ) and $T_{\rm g}$ of the neat polymer. The remaining VFTH parameters, B and τ_∞, are assumed not to change. Thus, in the LM model, the component segmental relaxation time is given by $\tau_{\rm seg}(\phi) = \tau_\infty \exp[B/(T - T_0(\phi))]$. Lodge and McLeish suggested that $\phi_{\rm self}$ should be calculated from the Kuhn length of the component. However, the $\phi_{\rm self}$ calculated does not work in most cases and it has to be treated as an adjustable parameter to yield agreement with experimental results [33–36]. Bedrov and Smith [31b] found for the LB-PBD component that only $\phi_{\rm self} = 0.0$ provides a better description of the α-relaxation times for the LB-PBD component in the 10% LB-PBD blend with CR-PBD, indicating that, within the LM formulation, the segmental relaxation of the fast component is determined entirely by the bulk composition of the blend. This is contrary to the spirit of the LM model which assumes that the local, dynamically relevant environment for a segment differs in composition from that of the bulk blend due to chain connectivity. The situation of the 50% LB-PBD blend is worse. Bedrov and Smith found even for the best case with $\phi_{\rm self} = 0.0$, the Lodge–McLeish model prediction still underestimates the slowing down of the α-relaxation of the LBPBD component. Roland *et al* [15, 16] applied the LM model to their data of the PVME/P2CS blends, and found that the modified Fox equation gives $\phi_{\rm self} = 0.437$ for the P2CS component, which is *less than* the actual concentration. The result contradicts the enrichment due to the intramolecularly bonded neighbouring segments. Moreover, one should not lose sight of the following facts on the LM model. First, the concept of self-concentration in the LM model does not apply to mixtures of small molecular glass-formers, and yet the component dynamics are similar to those of polymer blends. Second, ad hoc assumptions (e.g. the VFTH parameters, B and τ_∞, of the polymer in the blend being the same as those of the neat polymer, and the formula for $T_0(\phi)$) are made in arriving at the results of the model. Third, the use of the LM model is limited to fitting the segmental relaxation time of a component in the blend, and hence cannot address the other properties of the component dynamics discussed in this section. Fourth, the only link of the LM model to the glass transition problem is the empirical Fox equation on which it is based, and therefore it offers no help in understanding the more fundamental problem of the glass transition in the simpler case of a pure polymer. These shortcomings of the LM model do not seem to deter other workers on polymer blends from applying the model. This is because experimentalists would like to make comparisons of their measurements with theoretical predictions, and the LM model provides a prediction of $\tau_{\rm seg}(\phi)$. An effort could be made to make the CM more

appealing to experimentalists by making assumptions as bold as in the LM model. For example, the following assumptions can be made to arrive at a prediction of $\tau_{\mathrm{seg},A}(\phi)$ for component A in $\phi A/(1-\phi)C$ blends. (1) The primitive relaxation time of the component A, τ_{0A}, is the same as that of the pure A, which can be deduced from the VFTH fit to the segmental relaxation time of pure A by applying the CM equation and has been verified experimentally by measurements on polybutadiene [11]. (2) The most probable coupling parameter of component A in the blend, $\hat{n}_A$, is given by $\hat{n}_A = \phi_{\mathrm{eff}} n_A + (1-\phi_{\mathrm{eff}})(n_A + \Delta n_A)$, where ϕ_{eff} is calculated exactly from the chain parameters according to the expression given by LM, and Δn_A is an adjustable parameter. Finally, $\tau_{\mathrm{seg},A}(\phi)$ is calculated by $\tau_{\mathrm{seg},A}(\phi) = [t_c^{-\hat{n}_A}\tau_{0A}]^{1/(1-\hat{n}_A)}$. Assumption (1) is equivalent in spirit to the assumption of LM to use the B and τ_∞ parameters of the pure A for the component A in the blend. For polymer blends, we accept the concept of self-concentration of LM, and adopt the same formula proposed by them to calculate ϕ_{eff} from the chain parameters. Assumption (2) introduces Δn_A as the sole fitting parameter, equivalent in spirit to the LM model as letting ϕ_{eff} be adjustable. Thus, the assumptions made to calculate $\tau_{\mathrm{seg},A}(\phi)$ by the CM proposed here are no more or no less bold than those made by LM. With these assumptions, and Δn_A adjustable, the calculated $\tau_{\mathrm{seg},A}(\phi)$ may be in reasonable quantitative agreement with experimental data. Although this proposal may make the CM more appealing for workers in polymer blends to use, we will not propose it because the ad hoc assumptions made cannot be justified. The LM model and possibly this hypothetical proposal from the CM are attractive to some workers in polymer blends because they can predict $\tau_{\mathrm{seg},A}(\phi)$ from the known parameters of the pure polymer A and one adjustable parameter. However, since the factors determining the dynamics of the segmental relaxation and the VFTH temperature dependence of its relaxation time are not fully understood even for the pure polymer A, it is risky and overly ambitious to use phenomenology or empirical relations with unverifiable assumptions to predict quantitatively the segmental relaxation time of the same polymer when blended with another polymer.

6. Difference between chain diffusion dynamics and segmental dynamics of PEO in blends with PMMA

Neutron incoherent scattering and neutron spin echo experiments were reported by Wischnewski *et al* [37] on the Rouse-like diffusion of poly(ethylene oxide) (PEO, $T_g \approx 200$ K) chains in a miscible blend of PEO with poly(methyl methacrylate) (PMMA, $T_g \approx 400$ K). They found that the global dynamics of the fast PEO component in the blend is not determined by the average local environment of a polymer segment as it is commonly believed that segmental α-relaxation and global chain dynamics have the same temperature dependence. Actually, much stronger temperature dependence of the PEO chain diffusion coefficient than the PEO segmental relaxation time in blends with PMMA was found before. The tracer diffusion coefficient of unentangled poly(ethylene oxide) in a matrix of poly(methyl methacrylate) has been measured by Haley and Lodge [38]. The monomeric friction factor for the PEO tracers determined by diffusion was found to be a much stronger function of temperature than the corresponding PEO segmental dynamics measured at high frequencies by NMR. Over the *same* temperature range from 125 to 220 °C, the tracer diffusion coefficient changes by five orders of magnitude, while the segmental relaxation time of 3% up to 30% PEO in a matrix of poly(methyl methacrylate) changes by less than one order of magnitude [35] (see figure 2). This spectacular difference between the monomeric friction factors of the segmental relaxation and the tracer diffusion of PEO in a PMMA matrix is consistent with the findings of Wischnewski *et al* by neutron scattering in the same blends, and cannot be understood by conventional wisdom in viscoelasticity of polymers that all mechanisms have the same temperature dependence. The aforementioned behaviour of PEO in PMMA matrices is not

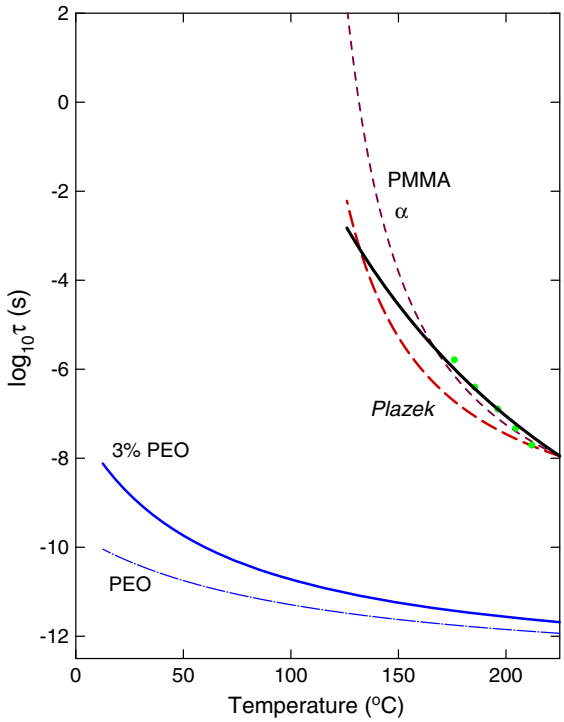

Figure 2. Comparison between the temperature dependences of the segmental relaxation time for (1) the PEO homopolymer (thin dashed–dotted line), and (2) 3% of PEO in PMMA (thick solid line) with that of (3) the dielectric segmental relaxation time of PMMA from Bergman *et al* (thin dashed line), (4) the terminal relaxation time of PMMA from Zawada *et al* shifted downward by 9.1 decades (open circles), (5) the shift factor of the softening dispersion of PMMA given by Plazek and co-workers shifted vertically downward by 0.82 decade to coincide with the dielectric segmental relaxation time at the highest temperature (thick dashed line), and (6) the monomeric friction factor of the PEO tracers in PMMA matrix from Haley and Lodge (continuous thick line).

found in polyisoprene/poly(vinylethylene) (PI/PVE) and blends. In the PI/PVE blends, global and local segmental motions of each component have been compared [33], and they exhibit about the same dependences on temperature. The many orders of magnitude difference of the friction factors of global and local segmental dynamics and their drastically different temperature dependences found for tracer PEO in a PMMA matrix, but not in the PI/PVE blends, poses yet another challenging problem in the component dynamics of polymer blends.

The segmental dynamics of PEO in PMMA was given an explanation before [27]. It was demonstrated that the predictions of the CM on the PEO dynamics in PEO/PMMA blends from 0.5% to 30% PEO are consistent with the experimental findings that $\tau_{\rm seg}$ of the PEO component is nearly composition independent over the entire composition range, and is retarded by less than one order of magnitude when compared with $\tau_{\rm seg}$ of pure PEO [35]. The cause of this unusual behaviour of $\tau_{\rm seg}$ of the PEO component is due to the high frequencies (31–76 MHz) used in the NMR measurements [35], resulting in primitive relaxation times τ_0 of the PEO component that are short and not much longer than the crossover time $t_{\rm c}$ of the CM [27]. The CM explanation of the unusual short-time segmental dynamics of PEO in the PEO/PMMA blends found by using NMR at high frequencies also applies to the similar short-time dynamics of PI in PI/PVE blends probed by the same high-frequency NMR technique [39] or by quasi-

elastic neutron scattering [40]. At such high frequencies, the segmental dynamics of PI is barely affected by blending with PVE.

The more recent PEO tracer diffusion measurements of Haley and Lodge [38] have uncovered yet another problem of the decoupling of the global dynamics from the segmental dynamics of PEO in PMMA. Needless to say, this problem and segmental dynamics problem of the PEO component in PMMA are related and have to be explained simultaneously. The diffusion of a tracer PEO chain in PMMA matrix involves global motion which is different from the local segmental relaxation in the nature and length-scale of the dynamics. The tracer PEO chain cannot diffuse without some motion of the matrix PMMA chains. Thus, the temperature dependence of the diffusion coefficient or the monomeric friction coefficient of the PEO tracer chain is determined by the motion of the matrix PMMA chains. The length-scale of the PMMA motion necessary for the PEO tracer to diffuse depends on the molecular weight of the PEO tracer. In figure 2 we reproduce for high molecular weight PMMA its dielectric segmental relaxation time [41], the shift factor of the Rouse dynamics in the softening dispersion measured by Plazek and co-workers [40] from 114 to 189 °C, and the shift factors of the entangled terminal dispersion obtained by Zawada *et al* [43] from 176 to 212 °C. These PMMA shift factors for motion at widely different length-scales, though different, all have much stronger temperature dependence than the segmental relaxation time of 0.5% to 3% of PEO in a PMMA matrix measured by high-frequency NMR [35]. For the low molecular weight unentangled PEO tracer used by Haley and Lodge [38], the shift factors of the PEO tracer diffusion coefficient may be closer to that of the Rouse dynamics of the PMMA matrix given by Plazek and co-workers because of compatible length-scales. It could be accidental, but nevertheless remarkable, that this Rouse dynamics shift factor of PMMA changes by about the same order of magnitude as the PEO tracer diffusion coefficient over the same temperature range, as shown in figure 2. Exact agreement is not expected between the temperature dependence of the PEO tracer diffusion coefficient and any of the shift factors of pure PMMA shown in figure 2.

From the considerations given above, we can rationalize why the PEO tracer diffusion dynamics have a much stronger dependence on temperature than the corresponding PEO segmental dynamics detected by high-frequency NMR in probe concentrations of PEO in a PMMA matrix. These results are unlike the PI/PVE blend systems in which global and local motions have been compared, and it was found that the segmental and terminal dynamics exhibited nearly the same dependences on temperature and composition [33]. For an explanation, let us consider the PI and the PVE component segmental dynamics measured by NMR at high frequencies and compare them with the longest global relaxation times determined by pulsed field-gradient NMR (PI) and rheology (PVE) in a common temperature range. The segmental relaxation times of PI and PVE in several blends including those of neat PVE and PI measured by Min *et al* [39] are reproduced in figure 3. The pulsed field-gradient NMR data for PI and rheology data for PVE have the same temperature and composition dependence [33], but are not shown in figure 3, for simplicity. To compare the temperature dependence of the same segmental and terminal dynamics of PI in 30% PEO/70% PVE blend (lower solid squares in figure 3) with those of PVE in the same blend, we shift the segmental relaxation time of PI (lower solid squares) vertically so that the shifted PI data (upper solid squares) coincide with the PVE data at high temperatures. By inspection, it is clear that the segmental and terminal dynamics of PI and PVE have nearly the same dependence on temperature throughout the range of measurements. Similar conclusions can be drawn for the other compositions. Therefore, in the PI/PVE blends, the diffusing PI chain sees all chains including PVE with dynamics having about the same temperature dependence at all length-scales from segmental to terminal. Naturally, the global relaxation time of PI has about the

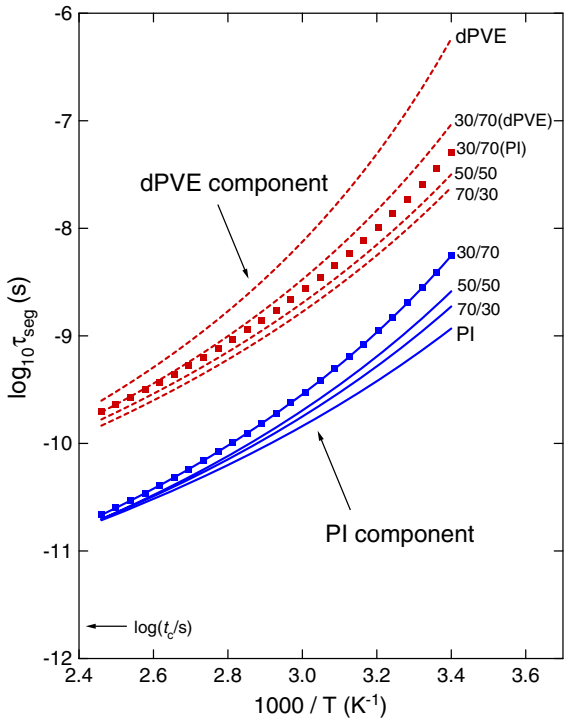

Figure 3. Segmental correlation times for both components in PI/PVE blends at various compositions. The data for the PI component in the 30% PI/70% PVE blend are shown by the line with solid squares on top of it. These data for PI are shifted vertically for the purpose of comparing with the temperature dependence of the segmental relaxation time of the PVE component in the same blend. For details, see text and figures in [33, 39].

same temperature dependence as its segmental relaxation time in the PI/PVE blends. The same argument holds for the PVE component. Hence, for each component, the ratio of the longest relaxation time to the segmental relaxation time is independent of both temperature and composition, as observed in experiments [33, 44]. The situation of the global dynamics of PI in PI/PVE blends is entirely different from the diffusion of PEO chains in PEO/PMMA blends, where at all length-scales the dynamics of PMMA have much stronger temperature dependences than the segmental dynamics of PEO.

7. JG β-relaxation, like α-relaxation, is sensitive to thermodynamic history and condition

We have seen from the discussions in section 2 that the ratio $\tau_{\rm JG}/\tau_\alpha$ is invariant for different T and P when τ_α is kept constant in many glass-formers. From this property alone, it can be inferred that, like τ_α, the JG relaxation time, $\tau_{\rm JG}$, has to be sensitive to pressure and temperature and the conjugate variables, volume and entropy. Two papers presented at the 4th WNEP [14, 45] reported obtaining different glass structures of the same glass-former by different thermodynamic paths. Starting at the some temperature T_i above $T_{\rm g}$ at ambient pressure, one path is first elevating the pressure to P_f until the liquid is transformed to a glass and then cooling the glass down to a final temperature T_f. A different path is to cool the liquid under ambient pressure from T_i to T_f at which the liquid is transformed to a glass, and then elevate the pressure up to P_f. Thus, the initial and final temperatures

and pressures are the same, but the two glasses have different densities. The interesting observation is that the JG relaxation time, τ_{JG}, differs by an order of magnitude or more in some glass-formers including *bis*-5-hydroxypentylphthalate and polyphenylglycidylether (PPGE). Even faster non-JG secondary relaxations such as that in phenolphthalein (PDE) show a dependence of its relaxation time on the thermodynamic path, but the change is significantly smaller [46]. Glasses such as dipropylene glycol dibenzoate obtained with different cooling rates also show a significant difference in τ_{JG}, and τ_{JG} increases with ageing [47]. Similar results were obtained for several other glass-formers [48]. These experimental facts about τ_{JG} all indicate that τ_{JG} is sensitive to density, ρ, just like τ_α. This property of τ_{JG} is expected by the CM because of the relation between τ_α and $\tau_0 \approx \tau_{JG}$ given by equation (2) now rewritten as $\tau_{JG}(\rho) \approx \tau_0(\rho) = [\tau_\alpha(\rho)]^{1-n} t_c^n$ to show explicitly the dependence of τ_{JG} on density. Several experiments on different glass-formers have shown that the dielectric strength of the JG relaxation, $\Delta\varepsilon_{JG}$, changes its temperature dependence near T_g [49, 50]. $\Delta\varepsilon_{JG}$ has a stronger temperature dependence above T_g than below T_g, which again indicates that the JG relaxation is sensitive to a change of the temperature dependence of density when crossing T_g.

The evidences presented above to show that τ_{JG} and its strength are dependent on density should have an impact on the controversy of whether or not τ_{JG} in the liquid state has the same Arrhenius temperature dependence as that of the glassy state [51–57]. Usually, near and above T_g, τ_{JG} and τ_α are not far apart and it is not possible to determine τ_{JG} without using some procedure. One procedure is the Williams hypothesis (often called the Williams Ansatz) that the total correlation function including the α and the β relaxations is $\varphi(t) = f_\alpha\varphi_\alpha(t) + (1 - f_\alpha)\varphi_\alpha\varphi_\beta(t)$. At the time Williams proposed his Ansatz, he did not have the benefit of recent experimental facts to distinguish β-processes that are JG secondary relaxations from non-JG secondary relaxations that are intramolecular in origin [7, 8]. The Ansatz was applied by others to resolve JG and non-JG secondary relaxations without distinguishing them, as for example those secondary relaxations considered in figures 1(a)–(f) of [52]. We now know that JG and non-JG secondary relaxations have distinctly different properties. JG relaxation has properties mimicking those of the α-relaxation, but not non-JG relaxation. An example is the pressure dependence of the JG relaxation time and the weaker pressure dependence or pressure independence of the non-JG relaxation time. Everyone seems to agree that the relaxation times, τ_β, of most if not all secondary relaxations have Arrhenius temperature dependence in the glassy state. However, some workers believe that the temperature dependence of τ_β in the liquid state has the same Arrhenius temperature as that of the glassy state when extrapolated to temperatures above T_g. This belief may hold for non-JG secondary relaxation, particularly those non-JG relaxations that are well separated from the α-relaxation, and its Arrhenius relaxation time line does not intersect the α-relaxation time line above T_g. Such non-JG relaxations are basically decoupled from the α-relaxation, and its Arrhenius temperature dependence can hold for its relaxation times above and below T_g. In fact, the secondary relaxations of PEA and PH shown in figures 1(a) and (b) of [52] are such trivial non-JG relaxations. For JG relaxation, we do not see how this belief can be consistent with the experimental evidences presented in the preceding paragraph that both its relaxation time τ_{JG} and strength $\Delta\varepsilon_{JG}$ are density dependent together with the well-known fact that the temperature dependence of the density in the liquid state is different from that in the glassy state. Moreover, the belief by some workers is entirely based on their use of the Williams Ansatz to fit dielectric spectra. However, the Ansatz of Williams at best is just a working hypothesis devoid of fundamental justification. Besides, there are cases in which the Williams Ansatz when applied still yields stronger temperature dependence of τ_{JG} above T_g than the Arrhenius temperature below T_g. An example is the application to the JG relaxation of 2-picoline in mixtures with tri-styrene [57]. In the case of the neat glass-formers sorbitol and xylitol, the JG relaxation

can be separated further apart from the α-relaxation by applying pressure. Consequently, at the elevated pressure of 1.8 GPa, the JG loss peak of sorbitol is completely resolved [56]. A similar situation is the JG relaxation of quinaldine in a mixture with 95% tri-styrene [13], which is well separated from the α-relaxation of quinaldine at T_g because τ_{JG} is shorter than τ_α by seven decades when $\tau_\alpha = 100$ s. The most probable τ_{JG} can be determined objectively from the frequency at the loss maximum in both cases without any need of using the William's Ansatz or other procedure to determine it at temperatures above T_g. The τ_{JG} so obtained clearly shows it has much stronger temperature dependence above T_g. Theoretical support of this behaviour comes from the CM equation (2), $\tau_{JG}(T) \approx \tau_0(T) = [\tau_\alpha(T)]^{1-n} t_c^n$. This equation indicates that τ_{JG} has Arrhenius temperature dependence below T_g because there τ_α is Arrhenius and n is temperature independent. Above T_g, again from the CM equation, τ_{JG} necessarily has a stronger temperature dependence as a consequence of the stronger VFTH temperature dependence of τ_α, and in general n if not constant would decrease with temperature.

Finally, in the Williams Ansatz, the α- and β-relaxations are assumed to be statistically independent of each other. Users of the Williams Ansatz to analyse experimental data must be aware that this assumption is incorrect at least when the β-relaxation is of the JG kind, as shown by new spin–lattice relaxation weighted stimulated-echo experiments of Böhmer and co-workers on several glass-formers [58]. The experimental data show a correlation between the α- and β-relaxations. As stated by Böhmer and co-workers, among theories and models of glass transition, the CM has a correlation between the α- and the JG β-relaxations. A more specialized and less specific approach than the CM was put forward by Cavaille *et al* [59]. From a quite different starting point these authors came along with an equation similar to the second relation of the CM (equation (2)), but t_c is treated as a floating parameter. Nevertheless, this approach by Cavaille *et al* also made a correlation between the α- and the JG β-relaxations, and hence this approach is consistent with the findings of Böhmer *et al* [58].

Let us return to the crossover of temperature dependence of the JG β-relaxation of the fast component (picoline [28, 57], tert-butylpyrindine (TBP) or quinaldine (QN) [13]) in blends with tri-styrene from Arrhenius temperatures dependence below T_{gf} to a stronger temperature dependence above T_{gf}, where T_{gf} is the glass transition temperature of the fast component. The crossover has been simply explained by the CM. Such crossover is seen for a resolved secondary relaxation of the PVME component in blends with 70% or more PS by Lorthioir *et al* [29]. For us, this is the JG β-relaxation of the PVME component in the blends. It was not resolved in neat PVME just like neat 2-picoline, TBP and QN. It becomes resolved when blended with PS, in exact analogy to mixing 2-picoline, TBP or QN with tri-styrene. This is due to increase in the coupling parameter n on blending with a less mobile component and the α- and the JG β-relaxations of the PVME are more separated as consequence of the CM relation, $(\log \tau_\alpha - \log \tau_{JG}) \approx n(\log \tau_\alpha + 11.7)$, discussed in section 4. On the contrary, due to the smaller value of n in neat PVME, the true intermolecular JG process is not resolved from the α-peak, and shows up as an excess wing. Lorthioir *et al* were not aware of these facts and the two resolved secondary relaxations of neat PVME (observed isochronally below 120 K at 1 Hz) are not the JG β-relaxation. Hence, they thought all secondary relaxations of neat PVME have been found, and the resolved process in blends with 70 and 80% PS (observed near 225 K isochronally at 1 Hz) is a new process which they call the α'-relaxation process. The mechanism they proposed to explain its origin is PVME segmental motion occurring in an environment consisting of 'frozen' PS chains. The shorter α'-relaxation time was explained as speeding up of the segmental α-relaxation of PVME in analogy to polymers confined to nanometre-scale dimension or dimensions. However, they also argued that PVME confined in such a frozen environment can only execute local conformational transitions and this is the α'-relaxation process they have in mind. Local conformational transition involving the entire repeat unit

of a polymer is basically the JG β-relaxation of any polymer, including PVME. Therefore, it is superfluous for Lorthioir *et al* to invoke new concepts in blends including 'frozen PS chains' and analogy to speeding up of relaxation by 'confinement' to arrive at essentially JG β-relaxation of PVME in the blends.

Lorthioir *et al* actually observed the α-relaxation of the PVME component in addition to the α'-relaxation or the JG β-relaxation in mixtures with 70% and 80% PS. For the 70% PS blend, the α-relaxation frequency $\nu_\alpha \equiv (1/2\pi\tau_\alpha)$ is 1 Hz at $T \approx 280$ K (see either figure 3 of [29a] or the coloured isochronal in figure 2 of [29b]). For some unknown reason, they did not plot any of the data for τ_α of the 70% PS blend on the Arrhenius plot in figure 7 of [29a] or figure 4 of [29b]. Had they put at least one data point ($1000/T = 3.57$, $\log(\tau_\alpha/s) = -0.8$) onto the plot, it would indicate the coexistence of the α-relaxation and the faster relaxation all coming from the PVME component. At the high concentration of 70% PS, τ_α of the PVME component is expected to have stronger temperature dependence (large steepness or fragility index) [21, 23]. This suggests that τ_α would reach 100 s at a temperature not too far below 280 K, T_{gPVME}, the glass transition temperature of the PVME component. Assuming that $T_{\mathrm{gPVME}} = 275$ K for the 70% PS blend, the corresponding reciprocal temperature, $1000/T_{\mathrm{gPVME}} = 3.64$, is near the location where the relaxation time of faster process crosses over from Arrhenius to a stronger dependence, as can be seen clearly from the inverted triangles in figure 4 of [29b]. This crossover of temperature dependence is exactly the same as that found for the JG β-relaxation of 2-picoline, TBP and QN in mixtures with tri-styrene, which further supports the identification of the faster process as the JG β-relaxation of PVME in the blends.

The interpretation by Lorthioir *et al* actually contradicts the Gaussian nature of concentration fluctuation of miscible polymer blends like PVME with PS. They stated that 'the molecular nature of this α'-relaxation has certainly to be related with the segmental α-relaxation of PVME, but in a constrained geometry'. This statement implies that the concentration fluctuations engender a bimodal distribution of PVME in the blend. One part of PVME is 'in a constrained geometry' giving rise to the α'-relaxation, and the other part is responsible for the α-relaxation. This contradicts the fact that the distribution of PVME caused by concentration fluctuation is Gaussian or nearly Gaussian in the miscible blend. Fluctuations leading to PVME being totally surrounded by less mobile PS can occur only in the tail of the Gaussian distribution and hence its contribution to the dielectric loss is small compared with the α-relaxation, in contradiction to experimental observation. The explanation of short α'-relaxation time as speeding up of the segmental α-relaxation of PVME in analogy to polymers confined to nanometre-scale dimension or dimensions is another assumption needed in order to explain the observed short relaxation time of the α'-relaxation. Although PS is less mobile, it still exerts a molecular interaction with the PVME. The situation here can be compared with the molecular dynamics simulation of the effect of a frozen Lennard-Jones (LJ) liquid acting as parallel walls confining the same LJ liquid [60, 61]. The frozen LJ particles still maintain an interaction with the LJ liquid near the interface like the less mobile PS on PVME, but the results of the simulation show that the α-relaxation of the confined LJ liquids near the frozen LJ walls is slowed down [60, 61] instead of speeding up, in contradiction to the assumption of Lorthioir *et al*.

8. Breakdown of Stokes–Einstein and Debye–Stokes–Einstein relations

The experimentally observed breakdown of the Stokes–Einstein and Debye–Stokes–Einstein relations was the subject of discussion in Round Table 1, and the current status of theoretical explanations proposed was reviewed by Richert [62]. Measurements of dynamics in glass-forming liquids indicate that the shear viscosity, η, the self-diffusion coefficient, D, and

the rotational correlation time, τ_c, all slow down dramatically with decreasing temperature. However, the products $D\eta$ and $D\tau_c$ are not constant but increase as the temperature is lowered towards T_g, as seen in 1,3-bis-(1-naphthyl)-5-(2-naphthyl)benzene (TNB) and other glass-formers [63–70]. Hence, there is enhanced translational diffusion, and the data do not satisfy the Stokes–Einstein (SE) and the Debye–Stokes–Einstein (DSE) relations. One explanation offered is based upon the spatially heterogeneous dynamics in supercooled liquids [63, 67]. It assumes that regions of differing dynamics give rise to the Kohlrausch relaxation function, $\exp[-(t/\tau_i)^{1-n_i}]$, in ensemble-averaging measurements. The decoupling between self-diffusion and rotation occurs because D and τ_c are averages over different moments of the distribution of relaxation times, with $D \propto \langle 1/\tau \rangle$ emphasizing fast dynamics, while $\tau_c \propto \langle \tau \rangle$ is determined predominantly by the slowest molecules. In order for this explanation to be consistent with the observed monotonic increases of the products $D\eta$ and $D\tau_c$ as the temperature is lowered toward T_g, the breadth of the relaxation time distribution has to increase (or the Kohlrausch exponent, $1 - n$, has to decrease) correspondingly. However, Richert and co-workers [65] recently reported that the dielectric spectra of TNB are characterized by a temperature-independent width (e.g. $(1 - n_d)$ is constant, equal to 0.50) from 345 to 417 K. The T_g of TNB is 342 K. Photon correlation spectroscopic and NMR [67] measurements all indicate a temperature-independent distribution of relaxation times. Similar results of enhanced translational diffusion and breakdown of SE and DSE relations but temperature-independent $(1 - n_d)$ were found in other glass-formers, including ortho-terphenyl [66], and in sucrose benzoate [69]. Thus, the data for TNB, ortho-terphenyl and sucrose benzoate contradict the explanation based on spatial heterogeneities.

A different explanation was offered by the CM [70, 71]. It was pointed out that the breakdown of the SE and DSE relations in glass-forming liquids are special cases of a more general phenomenon that different dynamic observables μ weight the many-body relaxation differently and have different coupling parameters n_μ (i.e., different degrees of intermolecular cooperativity) which enter into the stretch exponents of their Kohlrausch correlation functions,

$$\langle \mu(0)\mu(t) \rangle / \langle \mu^2(0) \rangle = \exp[-(t/\tau_\mu)^{1-n_\mu}]. \tag{3}$$

In the CM, the observed Kohlrausch relaxation time, τ_μ, is related to the primitive relaxation time, $\tau_{0\mu}$, by the relation

$$\tau_\mu(T) = [t_c^{-n_\mu} \tau_{0\mu}(T)]^{1/(1-n_\mu)}, \tag{4}$$

where $t_c \approx 2$ ps for molecular and polymeric glass-formers. Applying equation (4) to each observable μ we can immediately see that the observable having a larger n_μ will bestow a stronger temperature dependence for its relaxation time τ_μ. This is because the primitive relaxation times of all observables $\tau_{0\mu}$, uninfluenced by many-body relaxation dynamics, should have one and the same temperature dependence. To demonstrate enhanced translation diffusion by the CM, we need to know not only either n_η for viscosity, n_d for dielectric relaxation or n_{NMR} for NMR, but also n_D for diffusion. Unfortunately, for translational diffusion, so far only the diffusion constant, D, has been available from experiments. The complete time dependence of the correlation function for self-diffusion or probe diffusion of TNB, ortho-terphenyl and sucrose benzoate have not been measured, and n_D cannot be determined. Theoretical arguments have been given before [70] to show that n_η is larger than n_D, but this by no means settles the problem until experimental data prove it in the future. Nevertheless, assuming $n_D < n_\eta$ or $n_D < n_d$, from the CM equation (2) when applied to variables η or d for μ, and compared with that for variable D, it follows that $\tau_{\alpha\eta}$ or $\tau_{\alpha d}$ has a stronger temperature dependence than $\tau_{\alpha D}$. This is because in the CM all primitive relaxation

times, $\tau_{0\mu}$, have the same temperature dependence, i.e.,

$$\tau_{0D}(T) \propto \tau_{0d}(T) \propto \tau_{0\eta}(T). \tag{5}$$

Hence, we have an explanation of the breakdown of the SE and DSE relations. This CM explanation holds whether n_d and n_η are temperature dependent or independent as long as $n_D < n_\eta$ or $n_D < n_d$ [71]. In this manner, we have explained quantitatively for TNB the stronger temperature dependences of $\tau_{\alpha\eta}$ and $\tau_{\alpha d}$ than that of $\tau_{\alpha D}$ by taking a constant $n_\eta = n_d = 0.50$ as found by Richert and co-workers by dielectric relaxation measurements and assuming $n_D = 0.37$ [71].

In spite of the success, the undesirable and arbitrary assumption of a value of n_D less than n_η or n_d has to be made in order to explain the breakdown of the SE and DSE relations. A comprehensive experimental study of a supercooled molecular ionic liquid, 1-butyl-3-methylimidazolium hexafluorophosphate (BMIM-HFP), [bmim$^+$][PF6$^-$], by Ito and Richert [72] offers an opportunity to avoid making this assumption. This is because the molecules in ionic liquids are charged: their dynamics of translational diffusion can be fully characterized by ionic conductivity relaxation measurement as a function of frequency. The coupling parameter n_D is obtainable by fitting the frequency dependence of the ionic conductivity relaxation to the Fourier transform of the Kohlrausch function. Ito and Richert made isothermal conductivity relaxation measurements as a function of frequency on BMIM-HFP. From the data they deduced the electric modulus relaxation time, τ_M, and the coupling parameter $n_M = 0.49 \pm 0.05$. However, fitting the $M^*(\nu)$ data directly by the one-sided Fourier transform of the Kohlrausch function and emphasizing the good fit to the main peak of the electric loss modulus $M''(\nu)$ and its low-frequency flank yields a smaller $n_M \approx 0.41$. Since τ_M is proportional to τ_D and n_D is the same as n_M, from the conductivity relaxation data of Ito and Richert we can deduce n_D as well as the temperature dependence of τ_D. In addition, Ito and Richert measured the solvation dynamics and rotational dynamics of a probe molecule as a function of time. From the correlation functions they obtained the solvation and rotational relaxation times, $\tau_{\rm sol}$ and $\tau_{\rm rot}$, and the corresponding coupling parameters, $n_{\rm sol} = 0.70 \pm 0.03$ and $n_{\rm rot} = 0.63 \pm 0.05$. They showed that $\tau_{\rm sol}$ and $\tau_{\rm rot}$ follow the temperature dependence of η/T obtained by Xu *et al* [73] for more than ten decades, from sub-nanoseconds at room temperature to seconds near the glass transition temperature $T_{\rm g}$. On the other hand, τ_M (and hence τ_D) follows this trend only for temperatures $T > 1.2T_{\rm g}$, but its temperature dependence becomes significantly weaker than η/T in the $1.1T_{\rm g} > T > T_{\rm g}$ range. In fact, $\tau_D \propto \tau_M \propto \eta^{0.73}/T$, i.e., we have a fractional SE or DSE relation in the $1.1T_{\rm g} > T > T_{\rm g}$ range. This deviation is similar to the enhanced translational diffusion or fractional Stokes–Einstein behaviour observed in TNB, ortho-terphenyl and sucrose benzoate.

Both the values of $n_M \approx 0.5$ given by Ito and Richert, or the other possible value of $n_M \approx 0.41$, are smaller than $n_{\rm sol}$ and $n_{\rm rot}$. Either one of these two possible values of n_M can explain the enhanced translational diffusion. In fact, we can deduce at once from $n_{\rm sol} = 0.70 \pm 0.03$, $n_{\rm rot} = 0.63 \pm 0.05$ and $n_M = 0.49 \pm 0.05$ (or $n_M = 0.41$) that

$$\tau_M(T) \propto [\tau_{\rm sol}(T)]^{(1-n_{\rm sol})/(1-n_M)} = (\tau_{\rm sol})^{0.59} \tag{6}$$

and

$$\tau_M(T) \propto [\tau_{\rm rot}(T)]^{(1-n_{\rm rot})/(1-n_M)} = (\tau_{\rm rot})^{0.73}. \tag{7}$$

The fractional power in equation (7) is about the same as that observed. The one in equation (6) is smaller, but is not unacceptable considering the uncertainties of the values of both $n_{\rm sol}$ and n_M.

9. Nanoconfinement

Swenson and co-workers [74] reported that in highly confined water, like the 6 Å thick water layer in vermiculite clay and water in hydrated haemoglobin, they observed a relaxation with Arrhenius temperature dependence that could be the local β-relaxation of water. Since water is a very small molecule, the local β-relaxation must be its own JG relaxation. The phenomenon that the cooperative α-relaxation is transformed to the JG relaxation by nanoconfinement was found before in 1,2 diphenylbenzene (OTP) in 2 nm silanized glass pores [75], by Anastasiadis *et al* [76] in poly(methylphenyl siloxane) (PPMS) thin films by confinement in galleys of nanocomposites with width less than 2 nm, and by Schönhals and co-workers for poly(dimethyl siloxane) (PDMS) and poly(methylphenyl siloxane) (PPMS) confined in nanopores with size down to 2.5 nm [77, 78]. Additional evidences of the transformation include the change from Vogel–Fulcher–Tammann–Hesse temperature dependence to Arrhenius temperature dependence of the relaxation time with activation energy characteristic of JG relaxation [75–78], and the dielectric strength changes from decreasing with increasing temperature like that of α-relaxation to increasing with increasing temperature typical of JG relaxation [77, 78]. The relaxation times of PMPS thin films in nanocomposites and OTP and polymers confined in 2.5 nm glass pores are found to be close to the primitive relaxation time of the *bulk* glass-formers calculated by the CM equation from the known parameters n and τ_α of the bulk glass-formers [75, 79–81]. From this result, we can infer that the cooperative many-molecule dynamics of these glass-formers under extreme nanoconfinement are nearly totally suppressed, and that the observed relaxation times are those of the primitive relaxation or the JG β-relaxation of the nanoconfined liquid, which is closely related to but not necessarily identical to the JG β-relaxation of the *bulk* substances.

Torkelson [82, 83] used his fluorescence method to determine the nanoscale distribution of the glass transition temperature of nanoconfined polymer films layer by layer due to either enhancement or depreciation of molecular mobility by the presence of a free surface or a strongly attractive substrate respectively. The effects on molecular mobility of the free surface or the attractive substrate propagate layer by layer with attenuation into the polymer film. These results of Torkelson have been explained by the CM in a recent paper [84].

Peter reported [85] the results of molecular dynamics simulations for free-standing and supported thin films of a non-entangled polymer melt using a coarse-grained (bead-spring) model. The substrate is a non-attractive smooth wall and it also enhances the mobility of molecules nearby, although to a lesser degree than the free surface. They calculated the layer-resolved incoherent intermediate scattering function for a supported film. The data show that the monomer mobility is the highest at the free surface, it decreases monotonically as one goes towards the centre of the film, and at some point it increases monotonically again when approaching the smooth non-attractive wall. The layer-resolved intermediate scattering function as a function of time covers segmental relaxation at shorter times and internal chain dynamics at longer times and hence is more complicated than Lennard-Jones particles which have no chain modes. Nevertheless, the part of the decay of the layered-resolved intermediate scattering function due to segmental α-relaxation is most rapid at the free surface and becomes increasingly slower and more stretched out in time as one goes towards the centre. If it were possible to fit the time dependence of the segmental α-relaxation part of the layered-resolved intermediate scattering function by the Kohlrausch function, $\exp[-(t/\tau_j)^{1-n_j}]$, the trend may be described by simultaneous increases of τ_j and n_j, when going from the free surface layer to the central layer. Such simultaneous increase of τ_j and n_j would be consistent with the CM equation (2). The cooperative many-molecule α-relaxation dynamics of monomers in the surface layer are much more reduced than those in the bulk-like centre of the film due to the

absence of molecules on one side and reduction of intermolecular interaction and constraints acting on monomers at the surface. Hence the surface layer has a smaller coupling parameter, n_1, and a shorter relaxation time, τ_1, than either the central film or the bulk, a result that follows immediately from the CM equation. The accelerated dynamics of the monomers in the very first surface layer in turn have the effect of lessening the many-molecule α-relaxation dynamics of monomers in the next layer, although it is not as effective as air or vacuum on the surface layer. Hence the reduction of the coupling parameter is not as large as in the first layer. Hence, $n_1 < n_2 < n_{\text{central}} \leqslant n_{\text{bulk}}$, and it follows from the CM equation that $\tau_1 < \tau_2 < \tau_{\text{central}} \leqslant \tau_{\text{bulk}}$. Repeating the argument to inner layers, the trend exhibited by the layer-resolved intermediate scattering functions from simulation is recaptured by the CM. The same kind of explanation of simulation data for thin films had been done and published before [60] for films of binary Lennard-Jones liquid particles confined by parallel walls formed by frozen binary Lennard-Jones (LJ) particles [61]. The immobile LJ particles in the wall maintain their interaction with the confined LJ liquid. Since they are immobile, they further slow down the many-molecule relaxation in the first layer, resulting in an increase of the coupling parameter, n_1, over that of the central layer n_{central}. In the same spirit as the argument given before for the simulation of supported thin polymer films by Peter *et al*, we have $n_1 > n_2 > n_3 > \cdots > n_j > n_{j+1} > \cdots > n_{\text{central}}$, and it follows from the CM that $\tau_1 > \tau_2 > \tau_3 > \cdots > \tau_j > \tau_{j+1} > \cdots > \tau_{\text{central}}$ [60]. These expectations of the CM are realized in the simulations results of Scheidler *et al* [61], from which we find that each of the layer-resolved intermediate scattering functions is well fitted by the Kohlrausch function, $\exp[-(t/\tau_j)^{1-n_j}]$, and give n_j and τ_j in the process. This information enables a quantitative test of the CM in calculating τ_j from n_j using the CM equation, $\tau_j = [t_c^{-n_j}\tau_0]^{1/(1-n_j)}$, $t_c = 2$ units of LJ time, and τ_0 deduced from the simulation of the bulk binary LJ particles and used for all layers. The calculated τ_j are in accord with the simulation results within the uncertainties of the deduced values of n_j by Scheidler *et al*.

Torkelson's data do not give such detailed information as the intermediate scattering function from simulation, and hence no quantitative comparison can be made with the CM. Nevertheless, his data indicating that the effects of the free surface and the strongly attractive substrate propagate layer by layer into the polymer film are consistent with the CM results. Torkelson also reported that the size of the reduction of T_g of polymer thin films correlates with the 'fragility' or steepness index m of the polymer, apparently under the same conditions. For the family of amorphous polymers, m is proportional to n [86]. Hence his findings can be restated as a correlation between the size of the reduction of T_g with n. Rephrased this way, Torkelson's result could be consistent with the CM expectation because, from the CM equation, the change of segmental relaxation time is much larger for the polymer with larger n, for the same size of reduction of n by nanoconfinement.

Weeks [87] reported changes of colloidal particles dynamics by confining them between two parallel walls, and found that the particle motion is greatly slowed down. The extent of the slowing down increases immensely with increasing particle concentration, ϕ, shown by Weeks for three different samples. We recall from mean-square displacement and light scattering data for the same colloidal suspensions that n increases with ϕ [87, 88]. Thus, the observation of Weeks can be restated as follows. The extent of the slowing down of particle motion by confinement increases with increasing n of the unconfined colloidal suspension. One may recognize that this is just the analogue of (in the reverse direction) Torkelson's observation of increased reduction of T_g' of nanoconfined polymers with n. Both can be rationalized by the CM. There is even a closer analogy of the slowing down of colloidal particles by confinement with slowing down of the same system by ageing [89], which is clearly due to increase in

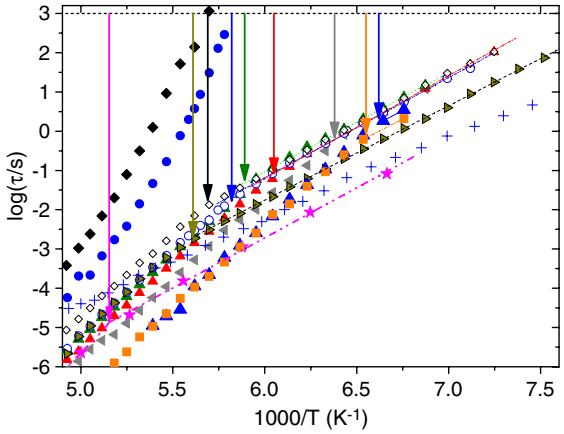

Figure 4. Relaxation map, $\log_{10}(\tau)$ versus $1000/T$, of the ν-process or the JG β-relaxation of water in various aqueous mixtures [91], and 6 Å thick water layer in a fully hydrated Na-vermiculite clay [96], and 50 wt% water in PVME [92]. The location of $1000/T_{gm}$ for each mixture is indicated by the vertical arrow pointing at the crossover where the relaxation time τ_ν changes temperature dependence from VFTH like above T_{gm} to Arrhenius below T_{gm}. Here T_{gm} is defined as the temperature at which the α-relaxation time of the mixture, τ_α, attains the long time of 10^3 s. The α-relaxation time τ_α is shown for two mixtures, 35 wt% water in PEG400 (black closed diamonds) and 35 wt% water in 6EG (blue closed circles). The crossover of temperature dependence of τ_ν at T_{gm} can be seen by the vertical arrow pointing downward at $\tau_\nu(T_{gm})$, the open diamond for 35 wt% water in PEG400, and open circle for 35 wt% water in 6EG. For the other mixtures, data for τ_α are not shown to avoid crowding. For the mixture of 35% water/PEG6, yellow right-pointing filled triangles represent τ_ν and the yellow arrow indicates the crossover at T_{gm}. For the mixture of 35% water in 3EG, the grey left-pointing filled triangles represent τ_ν, and the grey arrow indicates the crossover at T_{gm}. For the mixture of 35% water in 4EG, the red filled upward-pointing triangles represent τ_ν, and the red arrow indicates the crossover at T_{gm}. For the mixture of 35% water in 5EG, the green upward-pointing filled triangle represent τ_ν, and the green arrow indicates the crossover at T_{gm}. For the mixture of 40% water in 2EG, the blue filled triangles represent τ_ν, and the blue arrow on the extreme right indicates the crossover at T_{gm}. For the mixture of 40% water in glycerol, the filled orange squares represent τ_ν, and the orange arrow indicates the crossover at T_{gm}. For the mixture of 50% water/PVME, magenta filled stars represent τ_ν, and the magenta arrow on the extreme left indicates the crossover at T_{gm}. The blue crosses represent the relaxation time of 6 Å thick water layer in vermiculite clays.

n as shown in [71], while the structure was invariant [90] implying no observed increase in length-scale, a conclusion made by Weeks and co-workers [90].

10. JG relaxation of water

In the previous section we have mentioned that for several glass-formers, when nanoconfined to very small dimension or dimensions, the relaxation observed is devoid of many-molecule cooperativity and the α-relaxation becomes the local JG β-relaxation with relaxation time having Arrhenius temperature dependence. The 6 Å thick water layer in vermiculite clay [74] also shows a single relaxation with Arrhenius temperature dependence for its relaxation time over an extended temperature range from about 200 K down to 134 K (see figure 4). The activation energy is about 40 kJ mol^{-1}, which is approximately the energy required to break two hydrogen bonds of a water molecule. These properties indicate that the relaxation directly observed in the 6 Å thick water layer in vermiculite clay is the local JG β-relaxation of water.

Since bulk water crystallizes, the relaxation of water is often studied in mixtures with hydrophilic glass-formers that are susceptible to hydrogen bonding with water. These include

1-propanol, ethylene glycol (EG), ethylene glycol oligomers, poly(ethylene glycol) 400 and 600, fructose [91], tri-propylene glycol [92], and poly(vinylpyrro1idone) (PVP) [93, 94]. In these aqueous solutions, a faster relaxation is observed in addition to the slower relaxation by broadband dielectric relaxation. The slower relaxation has the VFTH-like temperature dependence of a primary α-process which is due to the cooperative motion of water and solute molecules hydrogen-bonded together that gives rise to the glass transition of the mixture, $T_{\rm gm}$, observed also by calorimetry (for two examples see figure 4). From the increase of its dielectric strength with water content in the mixtures [91], as well as the increase of its relaxation time, τ_ν, on replacing the protonated water by deuterated water [92], it is clear that the faster relaxations originate from water; these have been collectively referred to as the ν-process [91]. Its dielectric strength, $\Delta\varepsilon_\nu$, increases monotonically with temperature with an elbow shape that indicates a change of slope at $T_{\rm g}$ [91]. These properties are typical of secondary relaxation in neat glass-formers [49], and can be considered as another indication that the ν-process is the secondary JG relaxation of the water component in the aqueous mixtures.

At temperatures below $T_{\rm gm}$ of the mixture, τ_ν of all mixtures have Arrhenius temperature dependence with activation energies of around 50 kJ mol^{-1}, which is not too different from that of the JG β-relaxation observed in the 6 Å thick water layer in vermiculite clay, as demonstrated in figure 4. These properties of τ_ν are also indications that the ν-process in the aqueous mixtures are the local JG process of the water component. Although the ν-processes in various mixtures are non-cooperative JG relaxations of water, their τ_ν are not expected to have the same value because the concentrations as well the chemical structures of the other components are different. Nevertheless, the variations of τ_ν are within a few decades over extended temperature ranges where τ_ν are Arrhenius with about the same activation energy. Another general property of the ν-process is the change of temperature dependence of τ_ν near $T_{\rm gm}$ from the Arrhenius dependence below $T_{\rm gm}$ to stronger temperature dependence above $T_{\rm gm}$ [91–94]. This property is demonstrated in figure 4, where the vertical arrows indicate the locations of $1000/T_{\rm gm}$ as well as the location where τ_ν changes its temperature dependence in the aqueous mixtures. Here $T_{\rm gm}$ is defined as the temperature at which the α-relaxation time of the mixture, $\tau_{\alpha m}$, has attained the value of 10^3 s. It can be seen by close inspection that in general τ_ν changes its temperature dependence near $1000/T_{\rm gm}$. Such a change of temperature dependence of τ_ν has been found for the JG relaxation time, $\tau_{\rm JGf}$ of the fast component in several non-aqueous mixtures at the glass transition temperature, $T_{\rm gf}$, of the fast component [13, 28, 57, 95], and also in neat glass-formers [56]. Below $T_{\rm gf}$, the temperature dependence of $\tau_{\rm JGf}$ is Arrhenius, but it changes to stronger (VFTH-like) temperature dependence at higher temperatures after crossing $T_{\rm gf}$. Thus, the crossover of temperature dependence observed for τ_ν is analogous to that of JG relaxation in non-aqueous mixtures, and this common behaviour further supports the identification of the ν-process as the JG β-relaxation of the water component in aqueous mixtures. It can be seen by inspection of figure 4 that, for aqueous mixtures of comparable water concentrations, $\tau_\nu(T_{\rm gm})$ is shorter if $T_{\rm gm}$ of the mixture is higher. This trend is the same as that found in the fast component of non-aqueous mixtures discussed in section 4, and is expected by the CM because the coupling parameter of the fast component is larger if the mobility of the slower component is further decreased, or $T_{\rm g}$ of the slower component is higher. This crossover of τ_ν from VFTH-like to Arrhenius temperature dependence at $T_{\rm gm}$ was given a different explanation by Cerveny *et al* [92]. They explain the crossover as being due to water confined by the freezing of the aqueous mixture at temperatures below $T_{\rm gm}$, the same mechanism invoked by Lorthioir *et al* [29] to explain the origin of the faster relaxation of PVME in blends with PS with concentration of PS 70% and higher. At the end of section 7, we have presented facts and arguments to show that this explanation is unnecessary for the faster relaxation of the PVME component in the blends. By unnecessary, we mean the

introduction of the unproven concept of 'confinement' and the assumption that the enhanced mobility arises in the same manner as in glass-formers subjected to nanoconfinement, but the end result is local relaxation of PVME in the PVME/PS blends or local water molecule relaxation in the aqueous mixtures, which is no different from what we have identified as the JG β-relaxation of PVME or water. The explanation of the faster PVME relaxation in PVME/PS blends as being due to the effect of confinement by the 'frozen' PS is wrong, as explained in section 7. This similar argument used to explain the crossover of the temperature dependence of τ_ν at $T_{\rm gm}$ in aqueous solution is likely incorrect because $\tau_\nu(T_{\rm gm})$ generally becomes shorter on increasing the concentration of water [91, 92]. One would expect that the more stringent the confinement (the less water in the mixture), the larger would be the proposed effect, i.e., the relaxation time at the crossover, $\tau_\nu(T_{\rm gm})$, would be shorter. This expected behaviour from the effect of 'confinement' proposed contradicts the experimental results [91, 92].

If we know the coupling parameter, n, of bulk water, then we can take the observed JG β-relaxation time, $\tau_{\rm JG}$, of the 6 Å thick water layer in vermiculite clay approximately as the primitive relaxation time of bulk water and use the CM equation (2) to calculate the α-relaxation time, τ_α, of *bulk* water. This operation is opposite in direction to that used in [75, 79–81] on nanoconfinement to calculate $\tau_{\rm JG}$ from the known τ_α and n of the bulk glass-former. The coupling parameter, n, of bulk water is not known at temperatures below about 210 K. However, the Kohlrausch exponent $\beta_{\rm K}$ of bulk water at higher temperatures has been given by other workers. The values of $\beta_{\rm K}$ are 0.65 [96], and 0.60 [97, 98], from which the corresponding value of n are 0.35 and 0.40. Assuming that n continues to have these plausible values at lower temperatures, and $t_{\rm c} = 2$ ps, τ_α of bulk water is calculated from the $\tau_{\rm JG}$ of the 6 Å thick water layer in vermiculite clay by equation (2). The temperature at which the calculated $\tau_\alpha = 100$ or 1000 s is inferred as the glass transition temperature of bulk water. The results shown in figure 5 indicate that $T_{\rm g}$ of bulk water lies between 165 and 175 K [99][4]. This estimate of $T_{\rm g}$ of bulk water depends critically on the values of $\beta_{\rm K}$ given by others [96–98]. It is also possible that the actual n of bulk water or water in some other forms and configurations probed experimentally by others could be smaller. If this is true in any of these cases, then $T_{\rm g}$ can be much lower. For a demonstration, the arbitrary choice of $n = 0.10$ is also made in figure 5, and the calculated $T_{\rm g}$ is lower and near 136 K, the generally accepted $T_{\rm g}$ of water [100–102]. More experimental work has to be done before we can be sure of the true coupling parameter of bulk water and make a definite conclusion. The purpose of the exercise here in figure 5 is to demonstrate the potential use of the CM to deduce the $T_{\rm g}$ of bulk water. When the coupling parameter of bulk water is known with certainty, its $T_{\rm g}$ can be obtained. However, we are confident that the relaxation in the 6 Å thick water layer in vermiculite clay and the ν-process in aqueous mixtures presented in figure 4 are the JG β-relaxation of water in various environments. This result should have important implications on biomolecular function because of the role played by JG β-relaxation as emphasized by Frauenfelder in connection with protein dynamics [103].

11. Conclusion

During the 4th WNEP, the issue of the relevance of the theory and the model of the glass transition to experiments was raised. This is a timely issue because the field of the glass transition has basically been experimentally driven from the beginning until the present time. An abundance of experimental data has been accumulated for a variety of glass-forming

[4] For instance, $T_{\rm g} = 175$ K according to [92].

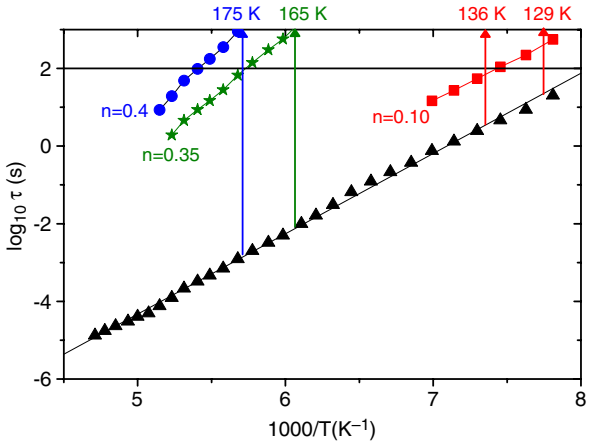

Figure 5. Relaxation map, $\log_{10}(\tau/s)$ versus $1000/T$, of water. Black filled triangles are the JG β-relaxation times from dielectric spectroscopy data for a 6 Å thick water layer in fully hydrated Na-vermiculite clay [74]. Blue filled circles, green stars and red squares are the cooperative α-relaxation time of bulk water calculated from the CM equation (2) with an assumed value of $t_c = 2$ ps, and τ_0 taken to be the same as the JG β-relaxation times of the 6 Å thick water layer, and $n = 0.4$, 0.35, and 0.1 respectively. Vertical arrows mark some of the values for T_g of bulk water proposed in the literature: for instance $T_g = 175$ K [92], $T_g = 165$ K from [99], $T_g = 136$ K from [100], and $T_g = 129$ K from [101].

substances waiting for theoretical treatment and explanation. Novel glass-formers as well as new experimental facts continue to be discovered every now and then. Thus it would be vain to entertain a theory of glass transition, no matter how mathematically rigorous or conceptually persuasive, if its relevance to experiments is limited or if it already contradicts general experimental results such as some of the ones discussed above.

The purpose of this paper is to show the broad relevance of the coupling model (CM) to experiments. This goal could have been accomplished by reviewing past accomplishments of the CM in explaining experimental data or explaining just one more new experimental fact. However, we have chosen a more challenging way to demonstrate the relevance of the CM to experiments by addressing a number of new experimental and computer simulation results reported and discussed at the 4th WNEP. Some of the new results have not been previously communicated in publication, and will appear in papers published in the same volume as the present paper and elsewhere.

Acknowledgments

The work at NRL was supported by the Office of Naval Research, and at the Università di Pisa by MIUR (PRIN 2005: 'Ageing, fluctuation and response in out-of-equilibrium glassy systems'). We thank Professor Naoki Shinyashiki for sending published data. KLN thanks Professor P A Rolla for hospitality during his stay at the Università di Pisa while this paper was written.

References

[1] Ngai K L 1979 *Comm. Solid State Phys.* **9** 141
[2] Ngai K L 1994 *Disorder Effects on Relaxational Processes* ed R Richert and A Blumen (Berlin: Springer) chapter 4

[3] Ngai K L and Tsang K Y 1999 *Phys. Rev.* E **60** 4511
[4] Ngai K L and Rendell R W 1997 *Supercooled Liquids, Advances and Novel Applications* (*ACS Symp. Series* vol 676) (Washington, DC: American Chemical Society) p 45
[5] Ngai K L 2001 *IEEE Trans. Dielectr. Electr. Insul.* **8** 329
[6] Ngai K L 2003 *J. Phys.: Condens. Matter* **15** S1107
[7] Ngai K L 2005 *J. Non-Cryst. Solids* **351** 2635
[8] Ngai K L and Paluch M 2004 *J. Chem. Phys.* **120** 857
[9] Ngai K L, Casalini R, Capaccioli S, Paluch M and Roland C M 2005 *J. Phys. Chem.* B **109** 17356
[10] Ngai K L, Casalini R, Capaccioli S, Paluch M and Roland C M 2006 *Adv. Chem. Phys. Part B, Fractals, Diffusion and Relaxation in Disordered Complex Systems* vol 133, ed Y P Kalmykov, W T Coffey and S A Rice (New York: Wiley) Chapter 10, p 497
[11] Casalini R, Ngai K L, Robertson C G and Roland C M 2000 *J. Polym. Sci. Polym. Phys. Ed.* **38** 1841
[12] Roland C M, Casalini R and Paluch M 2003 *Chem. Phys. Lett.* **367** 259
[13] Capaccioli S, Lucchesi M, Kessairi K, Prevosto D and Rolla P A 2006 *Paper L34 in Abstract Book of 4th WNEP*
Capaccioli S, Lucchesi M, Kessairi K, Prevosto D and Rolla P A 2007 *J. Phys.: Condens. Matter* **19** 205133
Capaccioli S, Kessairi K, Prevosto D, Lucchesi M and Ngai K L 2006 *J. Non-Cryst. Solids* **352** 4643
[14] Prevosto D, Capaccioli S, Sharifi S, Lucchesi M and Rolla P A 2006 *Paper A15 in Abstract Book of 4th WNEP*
[15] Roland C M, Casalini R and McGrath K J 2006 *Paper L16 in Abstract Book of 4th WNEP*
Roland C M, Casalini R and McGrath K J 2007 *J. Phys.: Condens. Matter* **19** 205118
[16] Roland C M, McGrath K J and Casalini R 2005 *Macromolecules* **38** 8729
[17] Alegria A, Gomez D and Colmenero J 2002 *Macromolecules* **35** 2030
[18] Zetsche A and Fischer E W 1994 *Acta Polym.* **45** 168
[19] Kamath A, Colby R H and Kumar S K 2003 *Phys. Rev.* E **67** 010801
[20] Lodge T P and McLeish T C B 2002 *Macromolecules* **33** 5278
[21] Roland C M and Ngai K L 1991 *Macromolecules* **24** 2261
Roland C M and Ngai K L 1992 *Macromolecules* **25** 363
Roland C M and Ngai K L 1995 *Macromolecules* **28** 4033
Roland C M and Ngai K L 2000 *Macromolecules* **33** 3184
Roland C M and Ngai K L 1992 *J. Rheol.* **36** 1691
[22] Alegria A, Colmenero J, Ngai K L and Roland C M 1994 *Macromolecules* **27** 4486
[23] Ngai K L and Roland C M 2004 *Rubber Chem. Tech.* **77** 579
[24] Ngai K L and Capaccioli S 2004 *J. Phys. Chem.* **108** 11118
[25] Psurek T, Maslanka S, Paluch M, Nozaki R and Ngai K L 2004 *Phys. Rev.* E **70** 011503
[26] Capaccioli S and Ngai K L 2005 *J. Phys. Chem.* B **109** 9727
[27] Ngai K L and Roland C M 2004 *Macromolecules* **37** 2817
[28] Blochowicz T and Rössler E A 2004 *Phys. Rev. Lett.* **92** 225701
[29a] Lorthioir C, Alegria A and Colmenero J 2003 *Phys. Rev.* E **68** 031805
[29b] Lorthioir C, Alegria A and Colmenero J 2003 *Eur. Phys. J.* E **12** S127
[30] Zhang S, Jin X, Painter P C and Runt J 2002 *Macromolecules* **35** 3636
[31a] Bedrov D and Smith G D 2005 *Macromolecules* **38** 10314
[31b] Bedrov D and Smith G D 2006 *Macromolecules* **39** 8526
[31c] Capaccioli S and Ngai K L 2007 *Macromolecules* to be submitted
[31d] Bedrov D and Smith G D 2006 *Eur. Polym. J.* **42** 3248
[32] Ngai K L, Capaccioli S and Roland C M 2006 *Macromolecules* **39** 8543 This is a Comment on [31a]
[33] Haley J C, Lodge T P, He Y, Ediger M D, von Meerwall E D and Mijovic J 2003 *Macromolecules* **36** 6142
[34] He Y, Lutz T R and Ediger M D 2003 *J. Chem. Phys.* **119** 9956
[35] Lutz T R, He Y, Ediger M D, Cao H, Lin G and Jones A A 2003 *Macromolecules* **36** 1724
[36] Lutz T R, He Y and Ediger M D 2005 *Macromolecules* **38** 9826
[37] Wischnewski A, Niedzwiedz K, Richter D, Genix A-C, Arbe A, Colmenero J, Straube E and Farago B 2006 *Paper L11 in Abstract Book of 4th WNEP*
[38] Haley J C and Lodge T P 2005 *J. Chem. Phys.* **122** 234914
[39] Min B, Qiu X, Ediger M D, Pitsikalis M and Hadjichristidis N 2001 *Macromolecules* **34** 4466
[40] Arbe A, Alegria A, Colmenero J, Hoffmann S, Willner L and Richter D 1999 *Macromolecules* **32** 7572
[41] Bergman R, Alvarez F, Alegria A and Colmenero J 1998 *J. Non-Cryst. Solids* **235–237** 580
[42] Ngai K L and Plazek D J 1996 *Physical Properties of Polymers Handbook* ed J E Mark (Woodbury, NY: American Institute of Physics) chapter 25, p 341
[43] Zawada J A, Ylitalo C M, Fuller G G, Colby R H and Long T E 1992 *Macromolecules* **25** 2896

[44] He Y, Lutz T R and Ediger M D 2004 *Macromolecules* **37** 9889
[45] Hensel-Bielowka S, Pawlus S, Plauch M, Ziolo J, Rzoska S J, Prevosto D and Sharifi S 2006 *Paper A20 in Abstract Book of 4th WNEP*
Hensel-Bielowka S, Pawlus S, Plauch M, Ziolo J, Rzoska S J, Prevosto D and Sharifi S 2007 at press
[46] Prevosto D, Capaccioli S, Lucchesi M, Rolla P A, Paluch M and Pawlus S 2006 *Phys. Rev.* B **73** 104205
[47] Prevosto D, Capaccioli S, Lucchesi M, Rolla P A and Ngai K L 2004 *J. Chem. Phys.* **120** 4808
[48] Capaccioli S, Lucchesi M, Kessairi K, Prevosto D and Rolla P A 2007 *Phys. Rev. Lett.* at press
[49] Johari G P, Powers G and Vij J K 2002 *J. Chem. Phys.* **116** 5908
Johari G P, Powers G and Vij J K 2002 *J. Chem. Phys.* **117** 1714
[50] Kudlik A, Benkhof S, Blochowicz T, Tschirwitz C and Rössler E 1999 *J. Mol. Struct.* **479** 201
[51] Bergman R and Svanberg C 2006 *Paper A2 in Abstract Book of 4th WNEP*
[52] Arbe A, Colmenero J, Gomez D, Richter D and Farago B 1999 *Phys. Rev.* E **60** 1103
[53] Donth E, Schröter K and Kahle S 1999 *Phys. Rev.* E **60** 1099
[54] Bergman R and Svanberg C 2005 *Phys. Rev.* E **72** 043501
[55] Fujima T, Frusawa H and Ito K 2002 *Phys. Rev.* E **66** 031503
[56] Paluch M, Roland C M, Pawlus S, Ziolo J and Ngai K L 2003 *Phys. Rev. Lett.* **91** 115701
[57] Blochowicz T 2003 *PhD Thesis* Logos Verlag, Berlin
[58] Böhmer R, Diezemann G, Geil B, Hinze G, Nowaczyk A and Winterlich M 2006 *Phys. Rev. Lett.* **97** 135701
[59] Cavaille J Y, Perez J and Johari G P 1989 *Phys. Rev.* **39** 2411
[60] Ngai K L 2002 *Phil. Mag.* B **82** 283
[61] Scheidler P, Kob W, Binder K and Parisi G 2002 *Phil. Mag.* B **82** 283
[62] Richert R 2006 *Presentation in Round Table 2 of 4th WNEP* It is also a subject for discussion in Round Table 1
[63] Cicerone M T, Wagner P A and Ediger M D 1997 *J. Phys. Chem.* B **101** 8727
[64] Ngai K L, Magill J H and Plazek D J 2000 *J. Chem. Phys.* **112** 1887
[65] Richert R, Duvvuri K and Duong L J 2003 *J. Chem. Phys.* **118** 1828
[66] Richert R 2005 *J. Chem. Phys.* **123** 154502
[67] Mapes M K, Swallen S F and Ediger M D 2006 *J. Phys. Chem.* **110** 507
[68] Chakrabarti D and Bagchi B 2006 *Phys. Rev. Lett.* **96** 187801
[69] Rajian J R, Huang W, Richert R and Quitevis E L 2006 *J. Chem. Phys.* **124** 014510
[70] Ngai K L 1999 *J. Phys. Chem.* B **103** 10684
[71] Ngai K L 2007 *Phil. Mag.* at press
[72] Ito N and Richert R 2006 *J. Phys. Chem.* B at press
[73] Xu W, Cooper E I and Angell C A 2003 *J. Phys. Chem.* B **107** 6170
[74] Swenson J, Jansson H and Bergman R 2006 *Paper OL2 in Abstract Book of 4th WNEP*
Swenson J, Jansson H and Bergman R 2006 *Phys. Rev. Lett.* **96** 247802
[75] Ngai K L 1999 *J. Phys.: Condens. Matter* **11** A119
[76] Anastasiadis S H, Karatasos K, Vlachos G, Manias E and Giannelis E P 2000 *Phys. Rev. Lett.* **84** 915
[77] Schönhals A, Goering H, Schick Ch, Frick B and Zorn R 2005 *J. Non-Cryst. Solids* **351** 2668
[78] Schönhals A, Goering H, Schick Ch, Frick B and Zorn R 2003 *Eur. J. Phys.* E **12** 173
Schönhals A, Goering H, Schick Ch, Frick B and Zorn R 2004 *Colloid Polym. Sci.* **282** 882
[79] Ngai K L 2002 *Eur. Phys. J.* E **8** 225
[80] Ngai K L 2003 *Eur. Phys. J.* E **12** 93
[81] Ngai K L 2002 *Phil. Mag.* B **82** 291
[82] Torkelson J M 2006 *Paper L20 in Abstract Book of 4th WNEP*
[83] Ellison C J and Torkelson J M 2003 *Nat. Mater.* **2** 695
[84] Ngai K L 2006 *J. Poly. Sci. Polym. Phys. Edn* **44** 2980
[85] Peter S, Meyer H and Baschnagel J 2006 *Paper L19 in Abstract Book of 4th WNEP*
Peter S, Meyer H and Baschnagel J 2006 *J. Poly. Sci. Polym. Phys. Edn* **44** 2951
[86] Ngai K L and Roland C M 1993 *Macromolecules* **26** 6824
[87] Weeks E R 2007 *Paper OL11 in Abstract Book of 4th WNEP*
Weeks E R 2007 *J. Phys.: Condens. Matter* **19** 205131
[88] Segre P N and Pusey P N 1996 *Phys. Rev. Lett.* **77** 771
[89] Courtland R E and Weeks E R 2003 *J. Phys.: Condens. Matter* **15** S359
[90] Cianci G C, Courtland R E and Weeks E R 2006 *Flow Dynamics*; *AIP Conf. Proc.* **832** 21
[91] Shinyashiki N, Sudo S, Yagihara S, Spanoudaki A, Kyritsis A and Pissis P 2007 *J. Phys.: Condens. Matter* **19** 205113
[92] Cerveny S, Schwartz G A, Alegría A, Bergman R and Swenson J 2005 *J. Chem. Phys.* **124** 194501
Cerveny S, Colmenero J and Alegría A 2006 *Phys. Rev. Lett.* to be published

[93] Jain S K and Johari G P 1998 *J. Phys. Chem.* **92** 5851
[94] Shinyashiki N and Yagihara S 1999 *J. Phys. Chem.* B **103** 4481
[95] Capaccioli S, Kessairi K, Prevosto D, Lucchesi M and Ngai K L 2006 *J. Non-Cryst. Solids* **352** 4643
[96] Swenson J, Jansson H, Howells W S and Longeville S 2005 *J. Chem. Phys.* **122** 084505
[97] Torre R, Bartolini P and Righini R 2004 *Nature* **428** 296
[98] Masciovecchio C, Santucci S C, Gessini A, Di Fonzo S, Ruocco G and Sette F 2004 *Phys. Rev. Lett.* **92** 255507
[99] For instance, $T_g = 165$ K according to Velikov V, Borick S and Angell C A 2001 *Science* **294** 2335
[100] For instance, $T_g = 136$ K, from Johari G P, Hallbrucker A and Mayer E 1987 *Nature* **330** 552
[101] $T_g = 129$ K, as reported by Hallbrucker A, Mayer E and Johari G P 1989 *J. Phys. Chem.* **93** 7751
[102] Debenedetti P 2003 *J. Phys.: Condens. Matter* **15** R1669
[103] Frauenfelder H 2006 *Paper PL3 in Abstract Book of 4th WNEP*
Fenimore P, Frauenfelder H, McMahon B and Young R D 2005 *Proc. Natl Acad. Sci.* **101** 14408